Struct Chem (2012) 23:1523–1531
DOI 10.1007/s11224-012-9957-6

ORIGINAL RESEARCH

Synthesis, structure, and photophysical property of series of Ln(III) coordination polymers with different carboxylato ligands (Ln = Sm, Eu)

Jing Jin · Xiuyan Wang · Yanying Li ·
Yuxian Chi · Shuyun Niu

Received: 25 October 2011 / Accepted: 24 January 2012 / Published online: 15 February 2012

Abstract Four Ln(III) coordination polymers, $\{[Ln_2(1,3\text{-}bdc)_3(H_2O)_4]\cdot DMF\cdot H_2O\}_n$ (Ln = Sm **1**, Eu **2**) and $[Ln_2(mal)_3(H_2O)_6]_n$ (Ln = Sm **3**, Eu **4**) ($1,3\text{-}H_2bdc$ = isophthalate acid, H_2mal = malonate acid), were hydrothermally synthesized and characterized by single-crystal X-ray diffraction, elemental analysis, IR spectra, UV–Vis–NIR absorption spectra, and fluorescence spectra. The structural analyses reveal that polymer **1** is a 3D coordination polymer. Its asymmetry unit contains two crystallographically independent Sm(III) ions, both are eight-coordinated. The $1,3\text{-}bdc^{2-}$ anions show three different coordination modes. The structure of polymer **2** is isomorphous with that of **1**. Polymer **3** is also a 3D coordination polymer, its asymmetry unit contains one Sm(III) ion, which is nine-coordinate. The mal^{2-} anions have two different coordination modes. The structure of polymer **4** is isomorphous with that of **3**. The luminescent study shows that polymers **1**, **2**, and **4** exhibit characteristic emission bands in the visible region, corresponding to the transitions of the Ln(III) ions. By comparison and analysis of luminescence, it is found that the incidence of the same ligand on the corresponding spectra of different Ln(III) ions is different, and the influence of different ligands on luminescence of the same Ln(III) ion is also very different.

Keywords Ln(III) coordination polymer · Synthesis · Crystal structure · Photophysical property

Introduction

Ln(III) coordination polymers, due to their fascinating structure and unique physical property, always attract more and more attentions. The study for features and application exploration of such polymers are mainly focused on the luminescence, magnetics, molecular recognition and separation, medical diagnosis, cell imaging, etc. [1–10]. The luminescence of Ln(III) coordination polymers originates from the *f–f* transitions of Ln(III) ions. The intrinsic disadvantage of the *f–f* transitions is that the absorption coefficient is lower, thus resulting in weak emission [11, 12]. However, this weak absorbance can be overcome and improved effectively by coordinating suitable ligands with the antenna effect to the Ln(III) ion [13–17]. Typical ligands, such as β-diketonate, porphyrin, fluorescein, 8-quinoline as well as their derivatives, have been demonstrated the successful sensitization to the luminescence of Ln(III) ion. Apart from sensitizing the luminescence of Ln(III) ions, the different ligands are crucial to generation of the fascinating structures. As far as carboxylate ligands, the flexible carboxylate ligands (such as succinate, malonic, citric acids, etc.), while usually making a small contribution to sensitization of luminescence of Ln(III) ions (even quenching the luminescence), is more favorable for generation of the novel architectures and topologies because of their rich conformation capable of meeting the requirement for coordination geometry of different Ln(III) ions [18–20]. For example, the suc^{2-} anion (H_2suc = succinate acid) can feature *cis-* and *trans*-conformations to assembly with Ln(III) ions, generating various coordination frameworks from 1D to 3D [21, 22]; the mal^{2-} anion (H_2mal = malonic acid) can adopt chair, boat, and envelope three conformations to bridge Gd(III) ions to form a 2D layer structure; curiously, in another Gd-mal polymers,

---

Electronic supplementary material The online version of this article (doi:10.1007/s11224-012-9957-6) contains supplementary material, which is available to authorized users.

J. Jin · X. Wang · Y. Li · Y. Chi · S. Niu (✉)
School of Chemistry and Chemical Engineering, Liaoning Normal University, Dalian 116029, People's Republic of China
e-mail: syniu@sohu.com

the mal^{2-} ligands only show chair and boat two conformations, but it can bridge the Gd(III) ions into a 3D framework structure [23, 24]. Compared with the flexible ligand, under common circumstance, the rigid carboxylic ligand with high degrees of conjugation (such as benzene carboxylic acid, pyridine carboxylic acid as well as their derivatives, etc.), can efficiently sensitize the luminescence of Ln(III) ions after coordinating to the Ln(III) ions, usually presenting long luminescence lifetime and high luminescence intensity as well as good stability [8, 25, 26]. Therefore, ascertaining the luminescence, the relationship between luminescence and structure for Ln(III) coordination polymers has an important significance for in-depth investigation on various properties and exploiting their practical applications. In this study, we report four Ln(III) coordination polymers with 3D extended structure bridged by isophthalato and malonato ligands, respectively. Their structures were determined by single-crystal X-ray diffraction. The luminescent property of polymers **1**–**4** in visible region was analyzed and assigned. The influence of ligands on emission spectra of Ln(III) ions is discussed.

Experimental

Materials and measurements

The salt of $Ln(NO_3)_3 \cdot 6H_2O$ was prepared by dissolving the corresponding lanthanide oxide compound (purity is 99.99%) in the excess nitric acid, and then naturally crystallizing. Other starting materials and reagents were AR and used as purchased. The elemental analyses were performed on a PE-2400 elemental analyzer. The crystal structures were determined with Bruker Smart APEX-II CCD X-ray single-crystal diffractometer. The FT-IR spectra were recorded in 4,000–220 cm^{-1} scopes on a JASCO FT-480 spectrometer with pressed KBr pellets technique. The diffuse reflectance absorption spectra were obtained in 200–2,500 nm scopes on a JASCO V-570 UV–Vis–NIR spectrometer. The excitation and emission spectra in UV–Vis region were measured with a JASCO FP-6500 fluorescence spectrometer.

Syntheses of the polymers

$\{[Sm_2(1,3\text{-}bdc)_3(H_2O)_4]\cdot DMF\cdot H_2O\}_n$ **1**

$Sm(NO_3)_3 \cdot 6H_2O$ (0.22 g, 0.5 mmol) was dissolved in aqueous solution (5.0 mL), to which a mixture of 1,3-H_2bdc (0.06 g, 0.35 mmol) and water (5.0 mL) was added under stirring and heating (50 °C). Then, to the resulting clear solution, an appropriate amount of 1.0 mol L^{-1} NaOH solution was added dropwise to adjust the pH value to about 6. While, some white precipitate occurred, but they were dissolved following addition of DMF solution (5 mL). Then, the final solution was transferred into a Teflon bottle sealed in an autoclave, which was heated at 90 °C for 120 h. After cooling to room temperature and a standing period of 3 days, the reaction solution was filtered and the brown-yellow block crystals were obtained, washed out with mother liquid, and dried out in the air. The yield was 39% (0.19 g) based on Sm. Calc. for $C_{27}H_{29}Sm_2NO_{18}$ **1** (Found): C, 33.91 (33.73); H, 3.06 (3.04); N, 1.46 (1.45)%. IR(KBr, cm^{-1}): 3407s, 3037w, 2929w, 2855w, 1650m, 1608s, 1599s, 1541s, 1480m, 1448m, 1395vs, 1278w, 1167w, 1103m, 823w, 747s, 707m, 654m, 535m, 425m.

Polymer **2** was synthesized by the same procedure as **1** except for the replacement of $Sm(NO_3)_3 \cdot 6H_2O$ with $Eu(NO_3)_3 \cdot 6H_2O$.

$\{[Eu_2(1,3\text{-}bdc)_3(H_2O)_4]\cdot DMF\cdot H_2O\}_n$ **2**

$Eu(NO_3)_3 \cdot 6H_2O$ (0.22 g, 0.5 mmol) were used. The colorless block crystals were obtained. The yield was 42% (0.20 g) based on Eu. Calc. for $C_{27}H_{29}Eu_2NO_{18}$ **2** (Found): C, 33.80 (33.62); H, 3.05 (3.03); N, 1.46 (1.45)%. IR(KBr, cm^{-1}): 3433s, 3035w, 2929w, 2857w, 1647m, 1608s, 1600s, 1544s, 1477w, 1449w, 1396vs, 1280w, 1170w, 1103m, 819w, 750s, 703m, 659m, 532m, 425m.

$[Sm_2(mal)_3(H_2O)_6]_n$ **3**

$Sm(NO_3)_3 \cdot 6H_2O$ (0.22 g, 0.5 mmol) was dissolved in aqueous solution (5.0 mL), to which a mixture of H_2mal (0.1 g, 1 mmol) and water (5.0 mL) was added under stirring and heating (50 °C), getting colorless solution. An appropriate amount of 1 mol L^{-1} NaOH solution was added dropwise to adjust the pH value to about 4. Then, the final solution was stirred for 10 min and transferred into a Teflon bottle sealed in an autoclave, which was then heated at 90 °C for 120 h. After cooling to room temperature and a standing period of 2 days, the reaction solution was filtered and the colorless block crystals were obtained, washed out with mother liquid, and dried out in the air. The yield was 40% (0.14 g) based on Sm. Calc. for $C_9H_{18}Sm_2O_{18}$ **3** (Found): C, 15.12 (15.04); H, 2.54 (2.52)%. IR(KBr, cm^{-1}): 3335vs, 2914w, 1699s, 1567vs, 1448s, 1382vs, 1277s, 1187m, 964s, 712m, 647m, 625m, 532w, 454m.

Polymer **4** was synthesized by the same procedure as **3** except for the replacement of $Sm(NO_3)_3 \cdot 6H_2O$ with $Eu(NO_3)_3 \cdot 6H_2O$.

$[Eu_2(mal)_3(H_2O)_6]_n$ **4**

$Eu(NO_3)_3 \cdot 6H_2O$ (0.27 g, 0.6 mmol) were used. The colorless block crystals were obtained. The yield was 45%

(0.19 g) based on Eu. Calc. for $C_9H_{18}Eu_2O_{18}$ **4** (Found): C, 15.05 (14.97); H, 2.53 (2.51)%. IR(KBr, cm^{-1}): 3342vs, 2912w, 1699s, 1570vs, 1448s, 1383vs, 1277s, 1186m, 964s, 710m, 647m, 622m, 532w, 457m.

Single-crystal structural determinations

X-ray single-crystal diffraction data for polymers **1–4** were collected on a Bruker Smart APEX-II CCD diffractometer at 293(2) K with Mo-Kα radiation ($\lambda = 0.71073$ Å) by ω scan mode. Empirical absorption corrections were applied to the data using the SADABS program. Structures were solved by the direct methods and refined by full-matrix least squares on F^2 using the SHELXTL version 5.1 [27]. All of the non-hydrogen atoms were refined anisotropically. The hydrogen atoms bound to carbon atoms were placed in calculated position and refined isotropically with a riding mode. Hydrogen atoms of coordinated water molecules were found via Fourier difference map, then restrained and refined isotropically. Hydrogen atoms of lattice water molecules did not find further, so they could not be introduced in the refinement, but were included in the structure factor calculation. All the structural calculations and drawings were generated with the SHELXL-97 crystallographic software package. The main crystallographic data and structural refinement parameters of polymers **1–4** are summarized in Table 1.

Results and discussion

Structural descriptions

Structural analysis shows that polymer **1** is a 3D coordination polymer. Its asymmetric unit comprises two crystallographically independent Sm(III) ions (Sm1 and Sm2), three 1,3-bdc^{2-} anions, four coordinated water molecules, one uncoordinated DMF molecule, and one lattice water molecule (Fig. 1). The Sm1(III) ion is coordinated by the eight O atoms from five different 1,3-bdc^{2-} anions and two coordinated water molecules, forming a distorted square antiprism geometry (Fig. S1a in Supplementary material). The bond lengths of Sm1–O are in the range of 2.362(3)–2.560(3) Å (Table S1 in Supplementary material). The Sm2(III) ion is also eight-coordinate with six O atoms from five different 1,3-bdc^{2-} anions and other two O atoms from two coordinated water molecules, forming a distorted square antiprism geometry (Fig. S1b in Supplementary material). The bond lengths of Sm2–O are in the range of 2.367(3)–2.538(3) Å (Table S1 in Supplementary material). The three crystallographically independent 1,3-bdc^{2-} anions bond to Sm(III) ions in three different coordination modes: I-type, II-type, and III-type, respectively (Fig. 2). Each of carboxylate groups of I-type 1,3-bdc^{2-} anion bridges two different Sm(III) ions (Sm1 and Sm2 ions) with a bridging bidentate mode in *syn–anti* configuration [28] (Fig. 2a). The separation of Sm1···Sm2 is 4.929 Å.

Table 1 Crystal data and structure refinement parameters for polymers **1–4**

Polymer	1	2	3	4
Empirical formula	$C_{27}H_{29}Sm_2NO_{18}$	$C_{27}H_{29}Eu_2NO_{18}$	$C_9H_{18}Sm_2O_{18}$	$C_9H_{18}Eu_2O_{18}$
Formula weight	956.23	959.43	714.93	718.15
Crystal system	Monoclinic	Monoclinic	Monoclinic	Monoclinic
Space group	$P2_1/c$	$P2_1/c$	$C2/c$	$C2/c$
a (Å)	13.3713(12)	13.3471(14)	17.1797(16)	17.1551(19)
b (Å), β (°)	17.9197(16), 133.543(4)	17.8963(19), 133.570(5)	12.3090(12),127.5540(10)	12.2767(13), 127.5340(10)
c (Å)	18.7864(12)	18.7773(14)	11.1501(10)	11.1298(12)
V (Å^3)	3262.9(5)	3249.7(5)	1869.3(3)	1858.8(3)
Z	4	4	4	4
D_C (g cm^{-3})	1.947	1.961	2.540	2.566
F(000)	1,864	1,872	1,360	1,368
μ (mm^{-1})	3.645	3.906	6.313	6.779
Reflns. collected	17,518	16,094	4,586	4,524
Ind. reflns. (R_{int})	6,384(0.0307)	5,712(0.0289)	1,647(0.0248)	1,639(0.0213)
Range of θ (°)	1.88–26.00	1.88–25.00	2.23–25.00	2.23–25.00
GOOF	1.057	1.067	1.227	1.254
R_1, wR_2 [$I > 2\sigma(I)$]	0.0293, 0.0728	0.0300, 0.0769	0.0368, 0.0970	0.0343, 0.0905
R_1, wR_2 (all data)	0.0372, 0.0760	0.0347, 0.0789	0.0382, 0.0979	0.0355, 0.0911

Each carboxylate group of II-type 1,3-bdc^{2-} anion chelates to one Sm(III) ion (Sm1 or Sm2) with chelating bidentate mode [28] (Fig. 2b). The two carboxylate groups of III-type 1,3-bdc^{2-} anion bridge two equivalent Sm(III) ions(Sm1 or Sm2 ions) with a bridging bidentate mode in *syn–anti* configuration[28], respectively(Fig. 2c). The separations of Sm1C···Sm1B and Sm2···Sm2D are 4.689 and 4.705 Å, respectively.

In the crystal of **1**, first, $[Sm(H_2O)_2]^{3+}$ cations are bridged by 1,3-bdc^{2-} anions with I-type and III-type coordination modes, forming three different binuclear units of $[Sm_2(1,3\text{-bdc})_2(H_2O)_4]$, named A, B, and C, respectively (Fig. S2 in Supplementary material). These binuclear units exhibit an ABCBABCB sequence along the *a* axis, forming a 1D chain (Fig. 3, Fig. S3 in Supplementary material). Second, the remaining carboxylate groups of intra-chain I-type 1,3-bdc^{2-} anions together with II-type 1,3-bdc^{2-} anions all coordinate to the Sm(III) ions from the adjacent chains along the *b* axis, building the 2D layers in the *ab* plane as shown in Fig. 4. Finally, these layers are further extended along the *c* axis through the III-type 1,3-bdc^{2-} anions with coordinate of Sm(III) ions from adjacent layers, generating the 3D network (Fig. S4 in Supplementary material). Uncoordinated DMF molecule and lattice water molecule adhere to the framework of polymer **1** through hydrogen bonds (Fig. S5 in Supplementary material), which contributes to the stabilization of crystal structure.

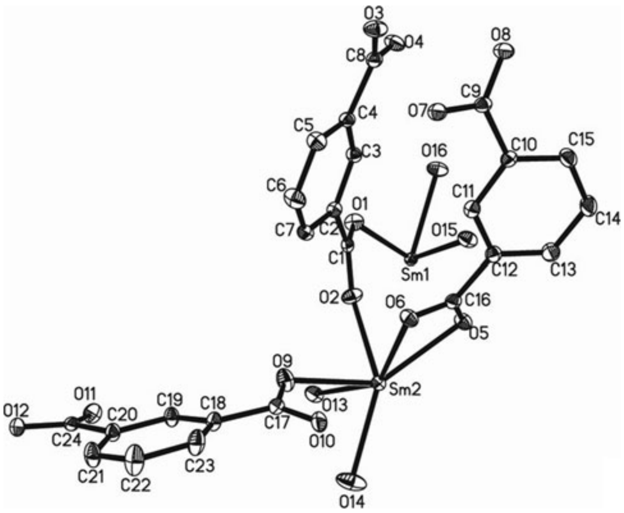

Fig. 1 Asymmetric unit of polymer **1** (free DMF and lattice water molecules are omitted for clarity)

The structure of polymer **2** is isomorphous with that of **1**, with the Eu(III) ion taking the place of the Sm(III) ion. The bond lengths of Eu1–O and Eu2–O are 2.351(4)–2.544(3) and 2.350(3)–2.528(3) Å, respectively (Table S1 in Supplementary material).

Polymer **3** is also a 3D coordination polymer. Its asymmetric unit comprises one Sm(III) ion, one and one-second mal^{2-} anions, and three coordinated water molecules (Fig. 5). The Sm(III) ion is nine-coordinate with six O atoms from four different mal^{2-} anions and three O atoms from three coordinated water molecules, forming a distorted monocapped square antiprism geometry (Fig. S6 in Supplementary material). The bond lengths of Sm–O are in the range of 2.319(5)–2.611(4) Å (Table S1 in Supplementary material). The mal^{2-} anions bond to Sm(III) ions in two different coordination modes, which are described as μ_2-mal^{2-} and μ_4-mal^{2-}, respectively (Fig. S7 in Supplementary material).

In the crystal of **3**, first of all, $[Sm(H_2O)_3]^{3+}$ cations are bridged by μ_2-mal^{2-} anions, forming a 1D chain along *b* axis (Fig. 6). Second, the 1D chains are further linked by one carboxylate group of μ_4-mal^{2-} anion in turn along *c* axis, resulting in formation of the 2D coordination layer in the *bc* plane as shown in Fig. 7. Finally, the left carboxylate groups of intra-layer μ_4-mal^{2-} ligands coordinate to the Sm(III) ions from neighboring layers, thus the 2D layers are linked in turn along *a* axis, building a 3D network (Fig. S8 in Supplementary material).

The structure of polymer **4** is isomorphous with that of **3**, with the Eu(III) ion taking the place of the Sm(III) ion. The bond lengths of Eu–O are 2.307(4)–2.605(4) Å (Table S1 in Supplementary material). These distances are comparable to the corresponding values of the reported Eu–mal complexes [29]. Although the structure of polymer **4** is

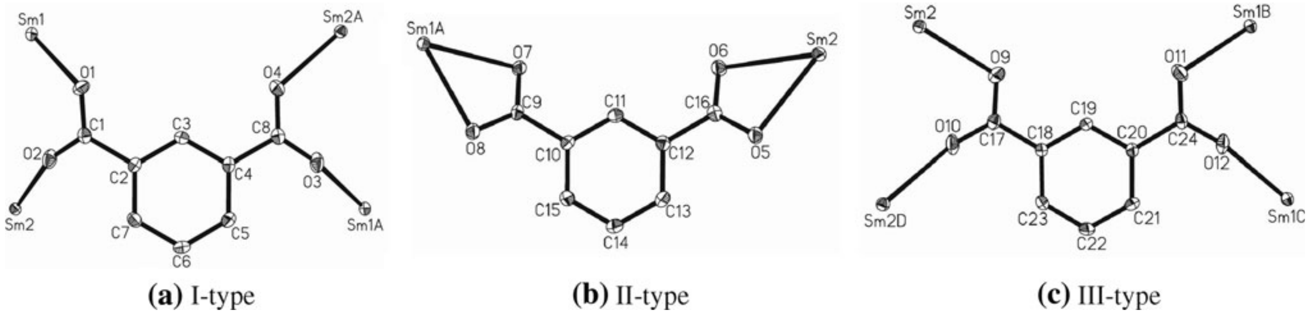

(a) I-type **(b)** II-type **(c)** III-type

Fig. 2 The coordination mode of three 1,3-bdc^{2-} anions with Sm(III) ions in **1**. The thermal ellipsoid is 30% probability. Symmetry code: *A* $-x + 1$, $y - 1/2$, $-z - 1/2$; *B* $-x + 2$, $-y$, $-z$; *C* $x + 1$, y, $z + 1$; *D* $-x + 1$, $-y$, $-z$

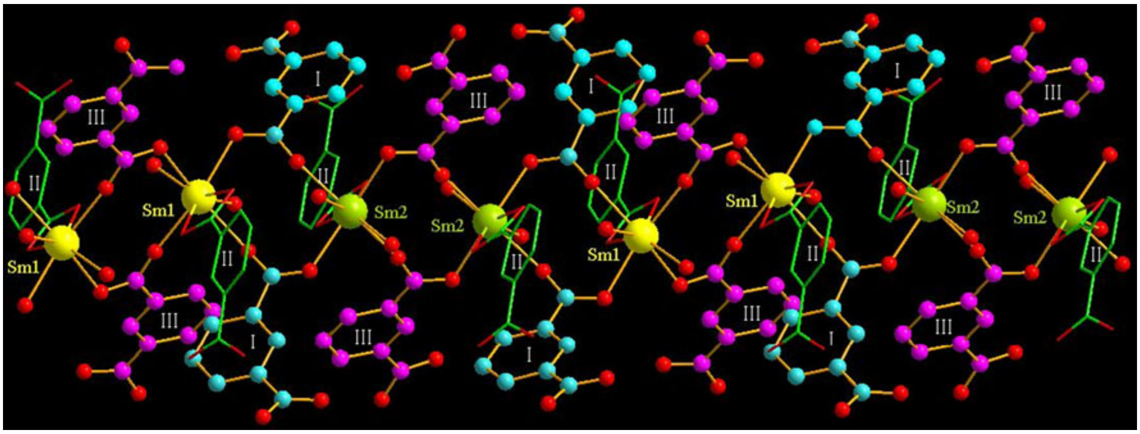

Fig. 3 The 1D chain of polymer **1** along *a* axis

Fig. 4 The 2D layer of polymer **1** in the *ab* plane (coordinated water molecules are omitted for clarity)

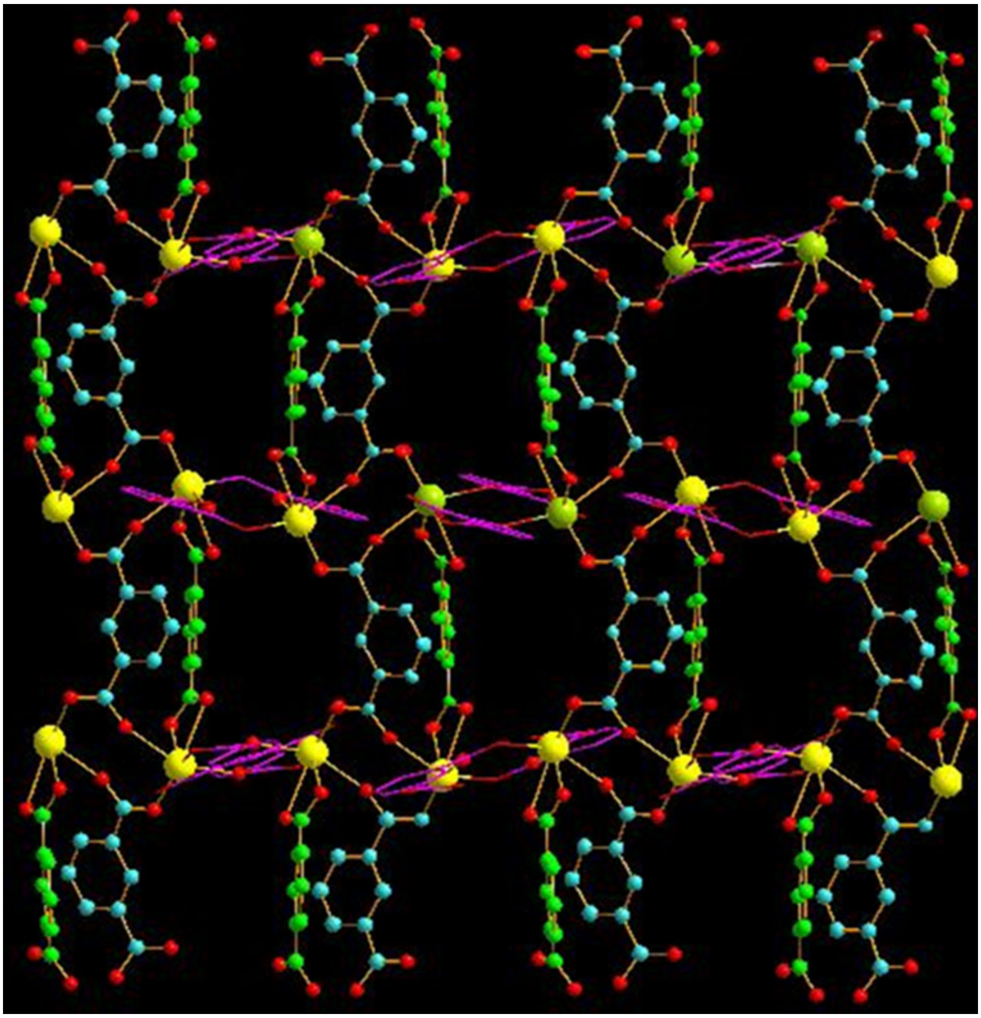

similar to that reported in the literatures [29, 30], the synthesis method, the crystal system and space group as well as property in this article are different from those reported. In this paper, we mainly focus on the luminescent properties of the four polymers, and the influence of structures of polymers on the luminescent properties.

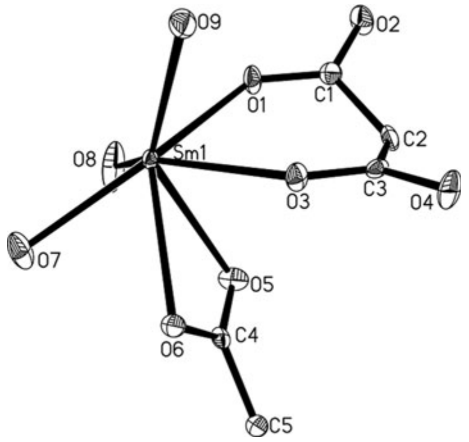

Fig. 5 Asymmetric unit of polymer **3** (hydrogen atoms are omitted for clarity)

Photophysical properties

UV–Vis–NIR absorption spectra

The UV–Vis–NIR absorption spectra of polymers **1**–**4** are shown in Fig. S9 in Supplementary material. The absorption spectra of the polymers **1** and **3** are composed the absorption bands of ligand and the *f*–*f* transition absorption bands of Sm(III) ions (Fig. S9a, c in Supplementary material). The absorption bands of ligand mainly lie in the ultraviolet region, while the *f*–*f* transition absorption bands of Sm(III) ion appear in the visible and near infrared region. The UV–Vis–NIR absorption spectra of polymers **2** and **4** are very similar (Fig. S9b, d in Supplementary material), composed of the absorption bands of ligand and the ligand-to-metal charge transition absorption bands (LMCT). They do not show the characteristic absorption bands of Eu(III) ions. The assignments of absorption spectra of four polymers and the corresponding ligands are listed in Table 2.

Fluorescence spectra

At room temperature, luminescence properties of the four polymers are investigated in the solid state.

With $\lambda_{\mathrm{Ex}} = 311$ nm, polymer **1** exhibits the characteristic emission bands of Sm(III) ion at 490, 546, and 589 nm (Fig. 8a), which can be ascribed to the $^4G_{5/2} \rightarrow {}^6H_J$ ($J = 5/2, 7/2, 9/2$) transition of the Sm(III) ion, respectively. The emission band from the transition ($^4G_{5/2} \rightarrow {}^6H_{7/2}$) is the strongest, which is similar to that in other Sm(III) complexes [31–33]. Compared with the theoretical emission bands of the Sm(III) ion [34] and the emission bands of other Sm(III) complexes reported [31–33], the emission bands of Sm(III) ion in polymer **1** present obviously blue-shift.

Polymer **2** reveals the characteristic emission bands of the Eu(III) ion upon excitation at 395 nm. As shown in Fig. 8b, the emission bands are attributed to $^5D_0 \rightarrow {}^7F_J$ ($J = 0, 1, 2, 3, 4$) transition, i.e., 579.5 nm ($^5D_0 \rightarrow {}^7F_0$), 589 and 592.5 nm ($^5D_0 \rightarrow {}^7F_1$), 613.5 and 619 nm ($^5D_0 \rightarrow {}^7F_2$), 652 nm ($^5D_0 \rightarrow {}^7F_3$), and 697 nm ($^5D_0 \rightarrow {}^7F_4$) [35, 36]. The emission band ($^5D_0 \rightarrow {}^7F_0$) is strictly forbidden in a field of symmetry, thus, the presence of which in polymer **2** reveals that the Eu(III) ion features a low-symmetry coordination environment [37, 38], in agreement with the result of X-ray single-crystal structural analysis. This is also reflected by the fact that the intensity ratio ($^5D_0 \rightarrow {}^7F_2/{}^5D_0 \rightarrow {}^7F_1$) in the solid state is high up to about 6.89, much higher than the value (0.67) for a centro-symmetric Eu(III) complex [37, 39]. The most intense transition is $^5D_0 \rightarrow {}^7F_2$, which implies a red emission light of **2**. The spectrum of polymer **2** is similar to those obtained for related Eu(III)–aromatic-carboxylate complexes [31, 38].

With $\lambda_{\mathrm{Ex}} = 300$ nm, the fluorescence spectra of polymer **3** is obtained (Fig. 8c). Only the characteristic emission bands of ligand appear in the range of 321–440 nm, while the emission bands of Sm(III) ion are not observed.

Upon excitation at 395 nm, polymer **4** shows the characteristic emission bands of Eu(III) ion (Fig. 8d). The bands at 579, 590, 613, 651, and 695 nm are attributed to the *f*–*f* transition of $^5D_0 \rightarrow {}^7F_J$ ($J = 0, 1, 2, 3, 4$), respectively. The most intense transition is also $^5D_0 \rightarrow {}^7F_2$. The presence of only one sharp peak in the region of the $^5D_0 \rightarrow {}^7F_0$ transition suggests the existence of a single chemical environment around the Eu(III) ion [40], which is in good agreement with the X-ray crystal structure of **4**. The emission spectrum of **4** is similar to that of Eu(III)–mal complex obtained at room temperature [29, 41].

The comparison and discussion of the luminescent properties of four polymers

Comparing and analyzing the emission spectra of polymers **1**–**4**, it can be found that

(1) The characteristic emission bands of the Ln(III) ions are observed in polymers **1** (Sm), **2** (Eu), and **4** (Eu),

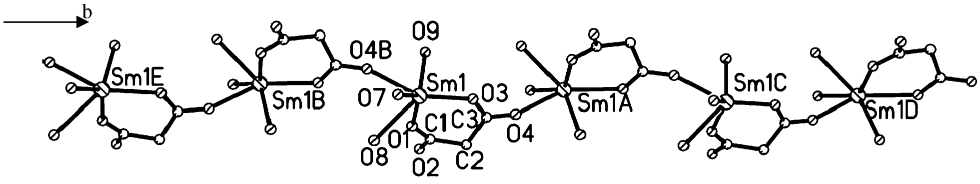

Fig. 6 The 1D chain of polymer **3** along *b* axis

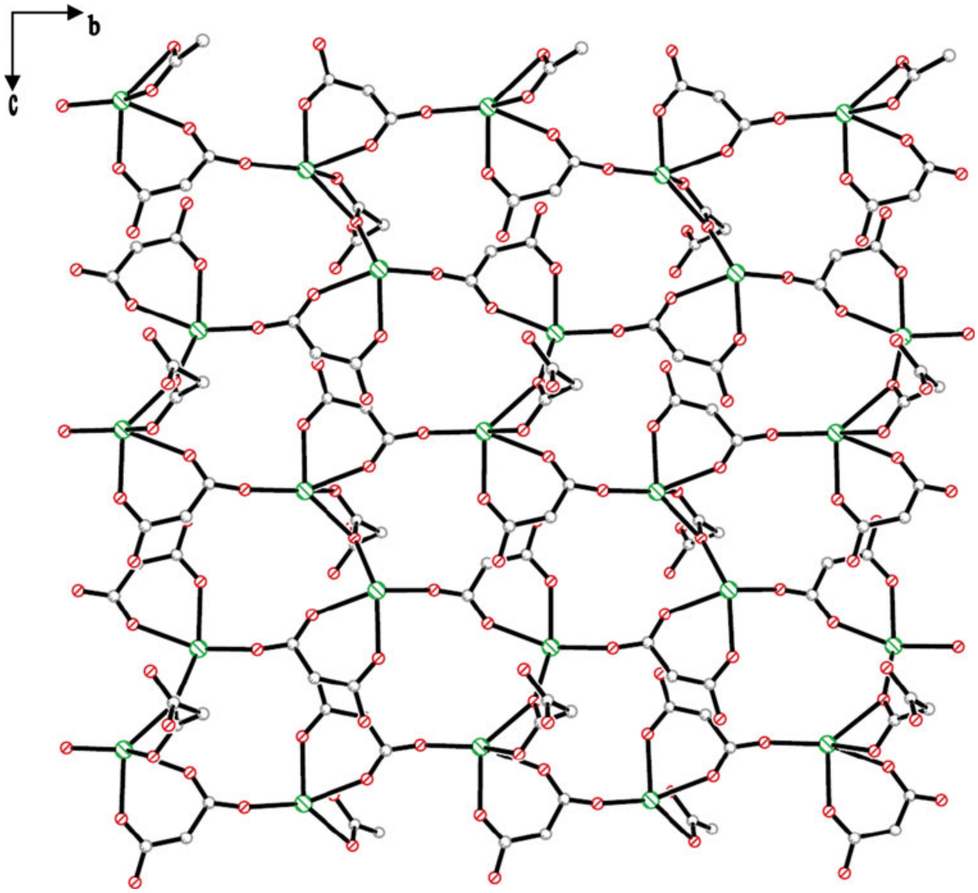

Fig. 7 The 2D layer of polymer **3** in the *bc* plane (coordinated water are omitted for clarity)

Table 2 The assignment of UV–Vis–NIR absorption spectra of polymers **1**–**4** and ligands

Polymer	Absorption (nm) (assignment)	Theoretical value [34] (nm)
1 (Sm)	1544, 1484, 1382, 1232, 1076, 940	1570, 1520, 1410, 1260, 1100, 955
	($^6H_{5/2} \rightarrow {}^6F_J$, $J = 1/2,3/2,5/2,7/2,9/2,11/2$)	
	436 ($^6H_{5/2} \rightarrow {}^4F_{5/2}$)	453
	314, 282, 254 (LLCT)	
2 (Eu)	398 (LMCT)	
	282, 262 (LLCT)	
3 (Sm)	1560, 1502, 1390, 1244, 1082, 942	1570, 1520, 1410, 1260, 1100, 955
	($^6H_{5/2} \rightarrow {}^6F_J$, $J = 1/2,3/2,5/2,7/2,9/2,11/2$)	
	478, 404 ($^6H_{5/2} \rightarrow {}^4F_J$, $J = 5/2,7/2$)	453, 404
	314, 256 (LLCT)	
4 (Eu)	392 (LMCT)	
	322, 258 (LLCT)	
1,3-H_2bdc	290, 248 (LLCT)	
H_2mal	208 (LLCT)	

while only the emission bands of ligand exist in polymer **3** (Sm). This indicates that the luminescence of Ln(III) ions in polymers **1**, **2**, and **4** get efficient sensitization from ligands.

(2) The same ligand shows different sensitization effects on luminescence of the different Ln(III) ions. For example, in polymers **1** (Sm) and **2** (Eu) bridged by 1,3-bdc^{2-} anion, although the 1,3-bdc^{2-} ligand efficiently sensitized the emissions of Sm(III) and Eu(III) ions with evidenced by quenching of the emissions of ligand (Fig. S10a in Supplementary material), the extent of the sensitization is different. In the same determination condition, even if the Ex. slit is (3, 3 nm) for polymer **1** and (3, 1 nm) for

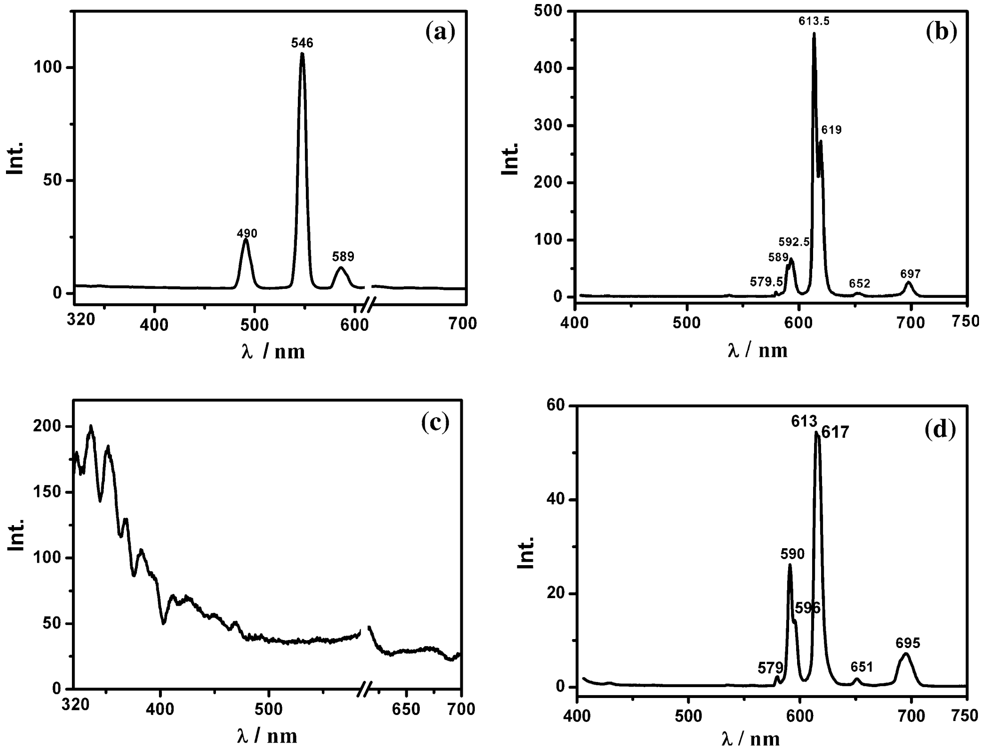

Fig. 8 The emission spectra of polymers **1**–**4**. **a** polymer **1** (Ex. slit: 3, 3 nm); **b** polymer **2** (Ex. slit: 3, 1 nm); **c** polymer **3** (Ex. slit: 3, 3 nm); **d** polymer **4** (Ex. slit: 3, 1 nm)

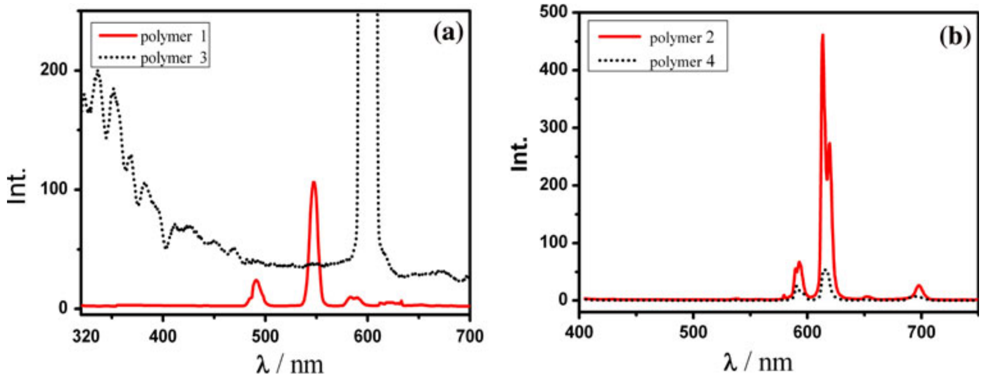

Fig. 9 Comparison of the emission spectra of polymers: **a** polymers **1** and **3**, **b** polymers **2** and **4**

polymer **2**, the emission intensity of polymer **2** is still much higher than that of polymer **1**. Similarly, for polymers **3** (Sm) and **4** (Eu), the mal^{2-} ligand only play the role of sensitization on the Eu(III) ions in polymer **4**. This may be due to that the emissive energy levels of different Ln(III) ions are different. This also was presented in other Ln(III) complexes reported [31].

(3) The incidence of the structure of ligands and the coordination environment of Ln(III) ions obviously affect the luminescence of Ln(III) ions. The conjugated extent of the ligand is better, the luminescence is stronger for corresponding ligand Ln(III) complexes. For example, the 1,3-bdc^{2-} ligand has rigid cyclo-conjugated structure, while the mal^{2-} ligand has not. Therefore, the emission intensity of polymer **2** is much stronger than that of polymer **4** under the same determination condition (the same λ_{Ex} and Ex. slit) (Fig. 9b). For polymers **1** and **3**, the emission bands of Sm(III) ion have not been observed in polymer **3** (Fig. 9a). This may be due to that the emissive energy levels of 1,3-bdc^{2-} ligand with π-conjugated structure are richer than that of mal^{2-} ligand, so they may match well with the emissive energy levels of Ln(III) ion (Fig. S11 in Supplementary material). In addition, reducing the number of coordinated water molecules around Ln(III) ions can also be helpful for their luminescence, which is due to decreasing the non-radiative energy loss [37]. For example, there are two coordinated water molecules around Ln(III) ion for polymers **1** and **2**, while there are three ones around Ln(III) ion for polymers **3** and

4. Therefore, the luminescence intensity of polymers **1** and **2** is stronger than that of polymers **3** and **4**, respectively.

Conclusions

Four Ln(III) coordination polymers [Ln = Sm (**1** and **3**); Eu (**2** and **4**)] were hydrothermally synthesized and structurally characterized by single-crystal X-ray diffraction. Polymers **1** and **2** are isostructural, which possess 3D structure bridged by 1,3-bdc^{2-} anion. Polymers **3** and **4** are also isostructural with 3D structure bridged by mal^{2-} anion. The luminescence study shows that polymers **1**, **2**, and **4** exhibit characteristic emission bands of corresponding Ln(III) ions benefiting from the sensitization of ligands; while polymer **3** mainly presents the emissions of ligand. By the comparative analysis of luminescence, it is found that the structure of ligand, species, and coordination environment of central metal ions all obviously affect the luminescence of Ln(III) ions.

Supplementary data

CCDC—848006 (for **1**), 848007 (for **2**), 848008 (for **3**), and 848009 (for **4**) contains the supplementary crystallographic data for this article. These data can be obtained free of charge via www.ccdc.cam.ac.uk/conts/retrieving.html (or from the Cambridge Crystallographic Data Centre, 12 Union Road, Cambridge CB21EZ, UK: Fax: + 44 1223 336033; or deposit@ccdc.cam.ac.uk).

Acknowledgment This study was supported by the National Natural Science Foundation of China (No. 20571037) and the innovational team project of Liaoning Province Educational Office (No. 2007T092).

References

1. Wang XJ, Cen ZM, Ni QL, Jiang XF, Lian HC, Gui LC, Zuo HH, Wang ZY (2010) Cryst Growth Des 10:2960–2968
2. Kitagawa S, Kitaura R, Noro S-I (2004) Angew Chem Int Ed 43:2334–2375
3. Pan L, Adams KM, Hernandez HE, Wang XT, Zheng C, Hattori Y, Kaneko K (2003) J Am Chem Soc 125:3062–3067
4. Radecka-Paryzek W, Kubicki M, Luks E (2010) Struct Chem 21:299–304
5. Wang P, Ma JP, Dong YB, Huang RQ (2007) J Am Chem Soc 129:10620–10621
6. Cañadillas-Delgado L, Fabelo O, Pasán J, Delgado FS, Lloret F, Julve M, Ruiz-Pérez C (2010) Dalton Trans 39:7286–7293
7. Dutra JDL, Gimenez IF, Costa NB Jr, Freire RO (2011) J Photochem Photobiol A 217:389–394
8. Sun YG, Rong ST, Yu W, Wu YL, Ding F, Gao EJ, Zhang WZ, Verpoort F (2009) Z Anorg Allg Chem 635:2585–2591
9. Wang HH, He P, Yan HG, Gong ML (2011) Sens Actuators B 156:6–11
10. Neves M, Gano L, Pereira N, Costa MC, Costa MR, Chandia M, Rosodo M, Fausto R (2002) Nucl Med Biol 29:329–338
11. Binnemans K (2009) Chem Rev 109:4283–4374
12. Xi P, Gu XH, Chen CF, He YX, Huang XA (2007) Spectrochim Acta A 66:667–671
13. Viswanathan S, de Bettencourt-Dias A (2006) Inorg Chem 45:10138–10146
14. Klink SI, Hebbink GA, Grave L, Oude Alink PGB, van Veggel FCJM (2002) J Phys Chem A 106:3681–3689
15. Hu M, Wang QL, Xu GF, Deng GR, Yang GM, Yu M, Zhang YH (2007) Inorg Chim Acta 360:1684–1690
16. Wu MF, Wang MS, Guo SP, Zheng FK, Chen HF, Jiang XM, Liu GN, Guo GC, Huang JS (2011) Cryst Growth Des 11:372–381
17. Dolbecq A, Dumas E, Mayer CR, Mialane P (2010) Chem Rev 110:6009–6048
18. Zhang LZ, Gu W, Li B, Liu X, Liao DZ (2007) Inorg Chem 46:622–624
19. Wu AQ, Zheng FK, Liu X, Guo GC, Cai LZ, Dong ZC, Takano Y, Huang JS (2006) Inorg Chem Commun 9:347–350
20. Amghouz Z, Roces L, García-Granda S, García JR, Souhail B, Mafra L, Shi F-N, Rocha J (2009) J Solid State Chem 182:3365–3373
21. Bernini MC, Garro JC, Brusau EV, Narda GE, Varetti EL (2008) J Mol Struct 888:113–123
22. Manna SC, Zangrando E, Bencini A, Benelli C, Chaudhuri NR (2006) Inorg Chem 45:9114–9122
23. Hernández-Molina M, Ruiz-Pérez C, López T, Lloret F, Julve M (2003) Inorg Chem 42:5456–5458
24. Cañadillas-Delgado L, Pasán J, Fabelo O, Hernández-Molina M, Lloret F, Julve M, Ruiz-Pérez C (2006) Inorg Chem 45:10585–10594
25. Gawryszewska P, Ciunik Z (2009) J Photochem Photobiol A 202:1–9
26. Lu WG, Jiang L, Lu TB (2010) Cryst Growth Des 10:4310–4318
27. Sheldrick GM (1997) SHELXS97 and SHELXL97. University of Göttingen, Göttingen
28. Deacon GB, Phillips RJ (1980) Coord Chem Rev 33:227–250
29. Hernández-Molina M, Lorenzo-Luis P, Ruiz-Pérez C, López T, Martín IR, Anderson KM, Orpen AG, Bocanegra EH, Lloret F, Julve M (2002) J Chem Soc Dalton Trans 2:3462–3470
30. Zhang CZ, Mao HY, Wang YL, Zhang HY, Tao JC (2007) J Phys Chem Solids 68:236–242
31. Huang YG, Wu BL, Yuan DQ, Xu YQ, Jiang FL, Hong MC (2007) Inorg Chem 46:1171–1176
32. Wang GL, Tian YM, Cao DX, Yu YS, Sun WB (2011) Z Anorg Allg Chem 637:583–588
33. An BL, Gong ML, Li MX, Zhang JM (2004) J Mol Struct 687:1–6
34. Gao JZ, Yang W, Kang JW (1995) Spectroscopic properties of the lanthanide complexes in aqueous solution. University of Electronic Science and Technology of China Press, Chengdu, pp 89–95
35. Zhuravlev KP, Tsaryuk VI, Pekareva IS, Sokolnicki J, Klemenkova ZS (2011) J Photochem Photobiol A 219:139–147
36. Subhan MA, Hasegawa Y, Suzuki T, Kaizaki S, Shozo Y (2009) Inorg Chim Acta 362:136–142
37. Liu TF, Zhang WJ, Sun WH, Cao R (2011) Inorg Chem 50:5242–5248
38. Daiguebonne C, Kerbellec N, Guillou O, Bünzli JC, Gumy F, Catala L, Mallah T, Audebr N, Gérault Y, Bernot K, Calvez G (2008) Inorg Chem 47:3700–3708
39. Klink SI, Grave L, Reinhoudt DN, van Veggel FCJM, Werts MHV, Geurts FAJ, Hofstraat JW (2000) J Phys Chem A 104:5457–5468
40. Biju S, Reddy MLP, Cowley AH, Vasudevan KV (2009) Cryst Growth Des 9:3562–3569
41. Martín IR, Lahoz F, Lavín V, Hernández-Molina M (2000) Opt Mater 25:223–229